



# Threshold photoelectron spectroscopy of the methoxy radical

Xiaofeng Tang, Xiaoxiao Lin, Gustavo A. Garcia, Jean-Christophe Loison, Christa Fittschen, Xuejun Gu, Weijun Zhang, Laurent Nahon

## ► To cite this version:

Xiaofeng Tang, Xiaoxiao Lin, Gustavo A. Garcia, Jean-Christophe Loison, Christa Fittschen, et al.. Threshold photoelectron spectroscopy of the methoxy radical. *Journal of Chemical Physics*, 2020, The Journal of Chemical Physics, 153 (3), 10.1063/5.0016146 . hal-02960901

**HAL Id: hal-02960901**

**<https://hal.univ-lille.fr/hal-02960901>**

Submitted on 18 Oct 2023

**HAL** is a multi-disciplinary open access archive for the deposit and dissemination of scientific research documents, whether they are published or not. The documents may come from teaching and research institutions in France or abroad, or from public or private research centers.

L'archive ouverte pluridisciplinaire **HAL**, est destinée au dépôt et à la diffusion de documents scientifiques de niveau recherche, publiés ou non, émanant des établissements d'enseignement et de recherche français ou étrangers, des laboratoires publics ou privés.

# Threshold photoelectron spectroscopy of the methoxy radical

Cite as: J. Chem. Phys. **153**, 031101 (2020); <https://doi.org/10.1063/5.0016146>

Submitted: 02 June 2020 . Accepted: 25 June 2020 . Published Online: 15 July 2020

Xiaofeng Tang , Xiaoxiao Lin, Gustavo A. Garcia , Jean-Christophe Loison , Christa Fittschen , Xuejun Gu, Weijun Zhang, and Laurent Nahon 



View Online



Export Citation



CrossMark

Lock-in Amplifiers  
up to 600 MHz



# Threshold photoelectron spectroscopy of the methoxy radical

Cite as: J. Chem. Phys. 153, 031101 (2020); doi: 10.1063/5.0016146

Submitted: 2 June 2020 • Accepted: 25 June 2020 •

Published Online: 15 July 2020



Xiaofeng Tang,<sup>1,a)</sup> Xiaoxiao Lin,<sup>1</sup> Gustavo A. Garcia,<sup>2</sup> Jean-Christophe Loison,<sup>3</sup> Christa Fittschen,<sup>4</sup> Xuejun Gu,<sup>1</sup> Weijun Zhang,<sup>1</sup> and Laurent Nahon<sup>2,a)</sup>

## AFFILIATIONS

<sup>1</sup>Laboratory of Atmospheric Physico-Chemistry, Anhui Institute of Optics and Fine Mechanics, HFIPS, Chinese Academy of Sciences, Hefei 230031, Anhui, China

<sup>2</sup>Synchrotron SOLEIL, L'Orme des Merisiers, St. Aubin, BP 48, 91192 Gif sur Yvette, France

<sup>3</sup>Institut des Sciences Moléculaires (ISM), CNRS, Univ. Bordeaux, 351 cours de la Libération, 33400, Talence, France

<sup>4</sup>University Lille, CNRS, UMR 8522, PC2A – Physicochimie des Processus de Combustion et de l'Atmosphère, F-59000 Lille, France

<sup>a)</sup>Authors to whom correspondence should be addressed: tangxf@aiofm.ac.cn and laurent.nahon@synchrotron-soleil.fr

## ABSTRACT

We present here a synchrotron radiation vacuum ultraviolet photoionization study of the simplest alkoxy radical, CH<sub>3</sub>O, a key reaction intermediate in atmospheric and combustion chemistry. A microwave discharge fast flow tube connected to a molecular beam sampling system is employed as a chemical reactor to initiate reactions and generate radicals. The CH<sub>3</sub>O<sup>+</sup> cation from direct ionization of the CH<sub>3</sub>O radical is detected successfully in the photoionization mass spectrum close to its ionization threshold. In addition, after identifying and removing the contribution of the <sup>13</sup>C-isotopic formaldehyde H<sub>2</sub><sup>13</sup>CO with the same isobaric mass  $m/z = 31$ , the high-resolution threshold photoelectron spectrum of CH<sub>3</sub>O is obtained and assigned with the aid of calculated Franck–Condon factors. The adiabatic ionization energy of CH<sub>3</sub>O is determined at 10.701 eV with an accuracy of 0.005 eV.

Published under license by AIP Publishing. <https://doi.org/10.1063/5.0016146>

## I. INTRODUCTION

Alkoxy radicals are key reaction intermediates and play essential roles in atmospheric and combustion chemistry.<sup>1</sup> In the atmosphere, they are formed by the oxidation of volatile organic compounds (VOCs) and can undergo isomerization, unimolecular dissociation, and bimolecular reactions, making them key players in the formation of secondary pollutants such as ozone and secondary organic aerosols.<sup>2–4</sup> The methoxy radical, CH<sub>3</sub>O, is the simplest and the most important alkoxy radical, mainly formed by the oxidation of CH<sub>4</sub> in the atmosphere. As a result, the kinetics, spectroscopy, and dynamics of CH<sub>3</sub>O have received a great deal of attention over the past decades.<sup>1,3</sup>

Various theoretical and experimental methods were applied to study the CH<sub>3</sub>O radical and its deuterated analog CD<sub>3</sub>O.<sup>5–9</sup> CH<sub>3</sub>O has a C<sub>3v</sub> symmetry in the X<sup>2</sup>E ground state with an electronic configuration of (1a<sub>1</sub>)<sup>2</sup>(2a<sub>1</sub>)<sup>2</sup>(3a<sub>1</sub>)<sup>2</sup>(4a<sub>1</sub>)<sup>2</sup>(1e)<sup>4</sup>(5a<sub>1</sub>)<sup>2</sup>(2e)<sup>3</sup>. The degenerate X<sup>2</sup>E ground state is subject to Jahn–Teller distortions along the

*e* vibrational modes, distorting into two C<sub>s</sub> symmetric states (<sup>2</sup>A' and <sup>2</sup>A''), with a splitting energy calculated at ~270 cm<sup>−1</sup>.<sup>10–12</sup> In ionization transitions, removing an electron from the outermost 2e orbital can generate the CH<sub>3</sub>O<sup>+</sup> cation into the X<sup>3</sup>A<sub>2</sub>, a<sup>1</sup>E, and b<sup>1</sup>A<sub>1</sub> states, where the singlet excited states are not stable and can rearrange to the isomer CH<sub>2</sub>OH<sup>+</sup>.<sup>5,7</sup>

The measurement of the ionization energy of CH<sub>3</sub>O appears to be very challenging due, for instance, to the presence of the CH<sub>2</sub>OH isomer that can contribute to the photoionization efficiency (PIE) curve. Ruscic and Berkowitz and Kuo *et al.* chose to turn toward deuterated CD<sub>3</sub>OH + F as a precursor to overcome this issue and found an adiabatic ionization energy (AIE) for CD<sub>3</sub>O of 10.726 ± 0.008<sup>8</sup> and 10.74 ± 0.02 eV<sup>5</sup> by photoionization mass spectrometry (PIMS). Ruscic and Berkowitz also derived a tentative photoelectron spectrum by differentiation of the modeled PIE.<sup>8</sup> Later, by HeI photoelectron spectroscopy (PES), the AIE of CH<sub>3</sub>O was reported at 10.72 ± 0.01<sup>6</sup> and 10.78 ± 0.02 eV.<sup>7</sup> Table I compiles the ionization energies available in the literature. Previous results show that

TABLE I. Adiabatic ionization energies (AIEs) of CH<sub>3</sub>O and related species.

Radicals	AIEs (eV)
CH <sub>3</sub> O	10.72(1), <sup>6</sup> 10.78(2), <sup>7</sup> 10.715(8), <sup>a</sup> 10.701(5) <sup>b</sup>
CD <sub>3</sub> O	10.72(1), <sup>6</sup> 10.74(2), <sup>5</sup> 10.726(8), <sup>8</sup> 10.729 <sup>c</sup>
CH <sub>2</sub> OH	7.56(1), <sup>17,18</sup> 8.14(1) <sup>d,17,18</sup>

<sup>a</sup>The calculated result with the ATcT recommended  $\Delta_f H_{0\text{K}}^0(\text{CH}_3\text{O}) = 28.85 \pm 0.29$  kJ mol<sup>-1</sup> and  $\Delta_f H_{0\text{K}}^0(\text{CH}_3\text{O}^+) = 1062.74 \pm 0.75$  kJ mol<sup>-1</sup>.<sup>19</sup>

<sup>b</sup>The present TPES result.

<sup>c</sup>The AIE of CD<sub>3</sub>O has been calculated in this work to be 28 meV above that of CH<sub>3</sub>O (see the text for details).

<sup>d</sup>The vertical ionization energy.

the CH<sub>3</sub>O<sup>+</sup> cation possesses, as the neutral, a C<sub>3v</sub> symmetric structure and that its optimized geometry is very similar to the one of the neutral CH<sub>3</sub>O radical, except for the C–O bond length, decreasing slightly from 1.386 Å to 1.309 Å upon ionization.<sup>9</sup> Therefore, the C–O stretching mode of CH<sub>3</sub>O<sup>+</sup> is expected to be excited upon ionization, and its vibrational frequency was theoretically predicted at 1279 cm<sup>-1</sup><sup>8</sup> and experimentally measured at 1950 cm<sup>-1</sup> by Zhu *et al.* via HeI PES.<sup>7</sup>

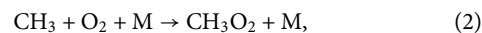
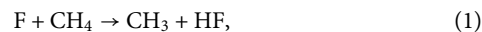
Photoelectron spectroscopy has been shown to give a more accurate picture of the spectroscopy of the cation than PIE<sup>13,14</sup> and also of the thermochemical values such as AIEs or appearance energies. Furthermore, modern threshold photoelectron spectroscopy provides a higher and constant resolution that can be used to give more precise and accurate values by comparison with *ab initio* methods. In this work, we present a vacuum ultraviolet (VUV) photoionization study of CH<sub>3</sub>O using double imaging photoelectron photoion coincidence (i<sup>2</sup>PEPICO) spectroscopy.<sup>15</sup> The mass-selected high resolution threshold photoelectron spectrum (TPES)<sup>14,16</sup> corresponding to the CH<sub>3</sub>O radical has been obtained, after removal of the H<sub>2</sub><sup>13</sup>CO contribution having the same isobaric mass. Then with the aid of the calculated Franck–Condon (FC) factors, the TPES has been assigned and the AIE of the CH<sub>3</sub>O radical is determined with a higher accuracy than previously reported values.

## II. EXPERIMENTAL SETUP

The experiments were performed on the undulator-based DESIRS beamline with the i<sup>2</sup>PEPICO spectrometer, DELICIOUS III, at synchrotron SOLEIL. The beamline configuration and the i<sup>2</sup>PEPICO spectrometer have been introduced previously, and only a brief description is provided here.<sup>15,20</sup> Synchrotron radiation photons, with linear horizontal polarization, were dispersed by a 6.65 m normal incidence monochromator from which a 200 l mm<sup>-1</sup> grating was adopted to provide high photon flux and energy resolution of ~3 meV with the chosen slit width. A gas filter located upstream of the beamline and filled with Ar was utilized to eliminate high harmonics from the undulator.<sup>20</sup>

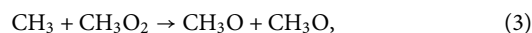
A fast flow tube mainly including a main tube and a collinear sliding injector was installed inside the source chamber of SAPHIRS, a permanent molecular beam end-station on the beamline, and acted as a chemical reactor to initiate reactions and generate radicals.<sup>21–23</sup> Fluorine atoms were produced from diluted F<sub>2</sub> gas in helium (5%, 10 SCCM) with a microwave discharge generator (2.45 GHz, Sairem

GMP03 KSM) and fed into the flow tube. After adding methane (30 SCCM) and oxygen (600 SCCM), together with helium carrier gas (1100 SCCM), the methyl radical (CH<sub>3</sub>) and the methyl peroxy radical (CH<sub>3</sub>O<sub>2</sub>) were produced through the reactions<sup>23</sup>



where M represents the species removing the internal energy of CH<sub>3</sub>O<sub>2</sub> by collisions. The pressure inside the flow tube was monitored by a capacity gauge and presently fixed at 2 Torr by a closed-loop feedback throttle valve.

Inside the flow tube, the bimolecular reaction between CH<sub>3</sub> and CH<sub>3</sub>O<sub>2</sub> and the self-reaction of CH<sub>3</sub>O<sub>2</sub> could generate the CH<sub>3</sub>O radical as follows:



This method avoids the presence of CH<sub>3</sub>OH as a precursor (contrary to using F + CH<sub>3</sub>OH),<sup>5,6,24</sup> which would make the measurements more challenging due to saturation (CH<sub>3</sub>OH having an ionization energy very close to that of CH<sub>3</sub>O).<sup>25</sup> The reaction of CH<sub>3</sub>O with O<sub>2</sub> will lead to HO<sub>2</sub>, while other radical–radical reactions such as the self-reactions of CH<sub>3</sub> and CH<sub>3</sub>O or the fast reaction of CH<sub>3</sub>O with HO<sub>2</sub> will also take place.<sup>4,26</sup> The major reactions undergoing in the flow tube are listed in Table S1.

After passing through two skimmers (1 mm diameter), the gas mixture in the flow tube was sampled and entered the ionization chamber of SAPHIRS, crossing the photon beam with a right angle.<sup>21–23</sup> The electrons and ions formed by photoionization at the center of DELICIOUS III were extracted and accelerated in opposite directions toward an electron velocity map imaging device and a modified Wiley–McLaren ion time-of-flight (TOF) 3D-momentum imaging analyzer and detected in coincidence via two position sensitive detectors (PSDs).<sup>15</sup> Electron images were filtered by the coincident ion mass-selection and position-selection to separate from background gas,<sup>21</sup> and an Abel inversion algorithm, pBasex, was utilized to provide the PES.<sup>27</sup>

## III. RESULTS AND DISCUSSION

Figure 1 shows the photoionization TOF mass spectrum integrated in the 9.7 eV–11.5 eV energy range. Almost all the species listed in Table S1, except those with ionization energies above 11.5 eV, have been detected. For example, the three intense peaks at *m/z* = 15, 30, and 47 are assigned as the CH<sub>3</sub> radical, formaldehyde (H<sub>2</sub>CO), and the CH<sub>3</sub>O<sub>2</sub> radical,<sup>23</sup> where H<sub>2</sub>CO can be produced from the CH<sub>3</sub>O + O<sub>2</sub>, CH<sub>3</sub> + CH<sub>3</sub>O, CH<sub>3</sub>O + CH<sub>3</sub>O<sub>2</sub>, and CH<sub>3</sub>O<sub>2</sub> + CH<sub>3</sub>O<sub>2</sub> reactions. The ethane (C<sub>2</sub>H<sub>6</sub>) product from the self-reaction of CH<sub>3</sub> leads to the same isobaric mass as H<sub>2</sub>CO, but its ionization energy located at 11.56 eV is beyond the present energy range so does not contribute to the *m/z* = 30 peak.<sup>25,28</sup> Other peaks are also observed in the mass spectrum and are assigned, i.e., *m/z* = 28 (ethene, C<sub>2</sub>H<sub>4</sub>), 32 (methyl alcohol, CH<sub>3</sub>OH), 46 (dimethyl ether, CH<sub>3</sub>OCH<sub>3</sub>), and 48 (methyl peroxide, CH<sub>3</sub>OOH).

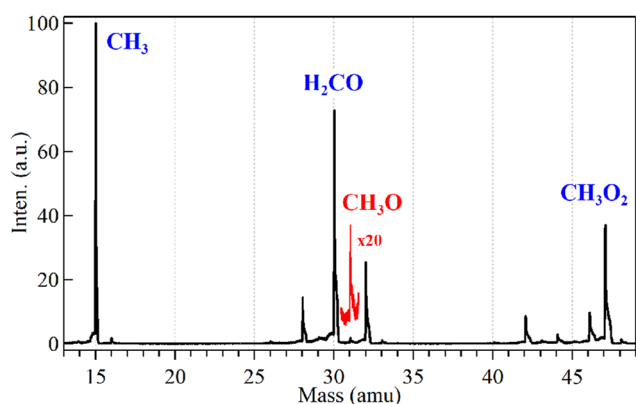


**FIG. 1.** Photoionization TOF mass spectrum integrated in the 9.7 eV–11.5 eV energy range, with 20 times magnified data in red to show the existence of  $\text{CH}_3\text{O}$ .

In particular, as shown in the magnified data in Fig. 1, the mass peak at  $m/z = 31$  is assigned as the  $\text{CH}_3\text{O}^+$  cation from direct ionization of  $\text{CH}_3\text{O}$ , close to its ionization threshold, although with a very weak signal. This channel carries contributions from  $\text{H}_2^{13}\text{CO}$ , and possibly from  $\text{CH}_2\text{OH}$ , although the energy range of this work precludes verification of the latter (see below).

The mass-selected photoelectron kinetic energy matrix corresponding to the  $m/z = 31$  cation, as a function of photoelectron kinetic energy (eKE) and photon energy, was measured by scanning the synchrotron photon energy with a step size of 10 meV and is presented in Fig. 2(a). The integration of the matrix over all photoelectron kinetic energies yields the PIE curve, which has been added

as a gray dashed line. As shown in Fig. 2(a), in the matrix, direct photoionization processes appear as a diagonal line with a unity slope,

$$eKE = h\nu - IE_{th}, \quad (5)$$

where  $IE_{th}$  is the ionization energy of a cationic state.

The mass-selected TPES is acquired by integrating the photoelectron signal  $A(h\nu, KE)$  along constant cationic states (diagonal lines), up to a maximum value  $KE_{max}$ , according to the following expression:<sup>29,30</sup>

$$TPES(h\nu) = \int_0^{KE_{max}} A(h\nu + KE, KE) dKE. \quad (6)$$

The TPES records the signal of near-zero kinetic energy photoelectrons ( $KE_{max} = 100$  meV) to get an intense signal, which is beneficial to the analysis of very diluted species, while its energy resolution ( $\sim 20$  meV) is comparable to that of the traditional TPES with subtraction of the hot electron contribution.<sup>13,31</sup>

Figure 2(b) shows the mass-selected TPES corresponding to the  $m/z = 31$  cation. As also visible directly from the matrix, two vibrational bands with their peaks at  $h\nu = 10.701$  eV and 10.880 eV are observed, the second band with a larger intensity than the first one in the TPES. Previous calculations show that the  $\text{CH}_3\text{O}^+$  cation possesses a similar structure as the neutral  $\text{CH}_3\text{O}$  radical,<sup>9</sup> so that the 0–0 adiabatic transition should correspond to the highest intensity peak in the PES. This is apparently not the case in the TPES of Fig. 2(b), whose unexpected shape therefore deserves a deeper analysis.

The hydroxymethyl radical ( $\text{CH}_2\text{OH}$ ) is the most stable isomer of the  $\text{CH}_3\text{O}$  radical, and it may contribute to the TPES too. However, the AIE and the vertical ionization energy (VIE) of  $\text{CH}_2\text{OH}$

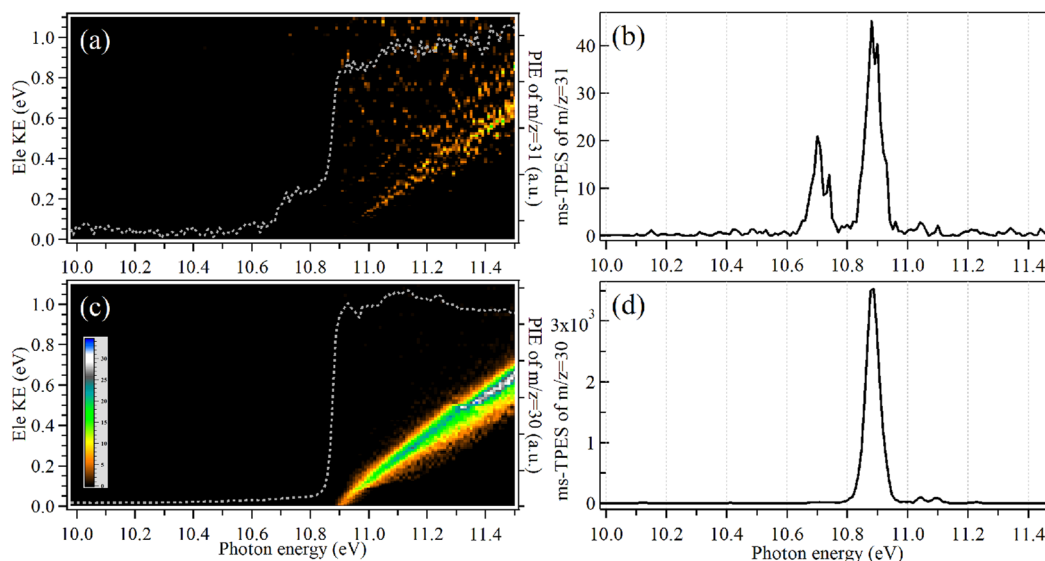


**FIG. 2.** Mass-selected photoelectron kinetic energy matrices and threshold photoelectron spectrum (TPES) corresponding to the [(a) and (b)]  $m/z = 31$  and [(c) and (d)]  $m/z = 30$  cations, together with their photoionization efficiency (PIE) curves marked with gray dashed lines. The inserted panel indicates that the signal intensity of the matrices increases from yellow to white, black being zero.

were measured at  $7.56 \pm 0.01$  eV and  $8.14 \pm 0.01$  eV,<sup>17,18</sup> respectively, far away from the present energy range. Moreover, the first excited state of  $\text{CH}_2\text{OH}^+$  (a triplet state) is calculated at 3.9 eV above the singlet ground state at the M06-2X/AVTZ level by using the *Gaussian* 16 program package,<sup>32</sup> so that a VIE of the excited state of  $\text{CH}_2\text{OH}^+$  would lie around 12 eV, more than 1 eV above the peaks we are observing. Therefore, the contribution of  $\text{CH}_2\text{OH}$  to our spectrum can be ruled out but not its presence in the reactor.

The  $^{13}\text{C}$ -isotopic formaldehyde  $\text{H}_2^{13}\text{CO}$  with a natural abundance of 1% of  $\text{H}_2^{12}\text{CO}$  has the same isobaric mass ( $m/z = 31$ ) as the  $\text{CH}_3\text{O}$  radical and might also contribute to the mass-selected TPES in Fig. 2(b). To demonstrate this, the mass-selected photoelectron kinetic energy matrix corresponding to formaldehyde ( $\text{H}_2\text{CO}$ ,  $m/z = 30$ ) was measured and is presented in Fig. 2(c). Figure 2(d) shows the mass-selected TPES of  $\text{H}_2\text{CO}$  in which an intense vibrational origin (0–0) peak is observed at  $h\nu = 10.890$  eV, in very good agreement with the literature AIE of  $\text{H}_2\text{CO}$  ( $\text{AIE} = 10.8887 \pm 0.0005$  eV).<sup>33</sup> The first band of the TPES of  $\text{H}_2\text{CO}$  therefore overlaps with the second band of Fig. 2(b), indicating that the  $^{13}\text{C}$ -isotopic formaldehyde  $\text{H}_2^{13}\text{CO}$  contributes to the mass-selected TPES of  $m/z = 31$  too.

By subtracting 1% of the TPES of  $\text{H}_2\text{CO}$ , i.e., the  $^{13}\text{C}$ -isotopic formaldehyde  $\text{H}_2^{13}\text{CO}$  contribution, from the mass-selected TPES of  $m/z = 31$  and assuming a constant ion detection efficiency between  $m/z = 30$  and  $m/z = 31$ , the TPES of the  $\text{CH}_3\text{O}$  radical without interferences from other species was retrieved, as presented in Fig. 3(a). Two vibrational bands can be observed in the TPES with now, after subtraction, a reduced intensity of the second band, coherent with the expected Franck–Condon factor-driven vibrational distribution. Note that the subtraction induced a slightly worse signal-to-noise ratio due to the weakness of the  $\text{CH}_3\text{O}$  radical signal with respect to the  $\text{H}_2\text{CO}$  one, and a spurious dip in the signal, marked with a blue star in the TPES.

To help assign the TPES of the  $\text{CH}_3\text{O}$  radical, the Franck–Condon factors for ionization transitions have been calculated at the M062X/aug-cc-pVTZ level of theory by using the *Gaussian* 16 program package<sup>32</sup> and are listed in Table II. The simulated PES is obtained by convolving the stick spectrum with a *Gaussian* function ( $\text{FWHM} = 40$  meV), as shown in Fig. 3(b). To match the experimental TPES, the calculated Franck–Condon factor-based stick PES and the simulated PES have been energetically shifted by 64 meV from the calculated AIE (10.637 eV).

As shown in Fig. 3, the agreement between the simulated PES and the experimental TPES is satisfactory and confirms that the  $m/z$  31-filtered and “purified” TPES corresponds to the  $\text{CH}_3\text{O}$  radical alone. Some differences between the simulated and experimental band intensities are seen for photon energies above 10.9 eV. While

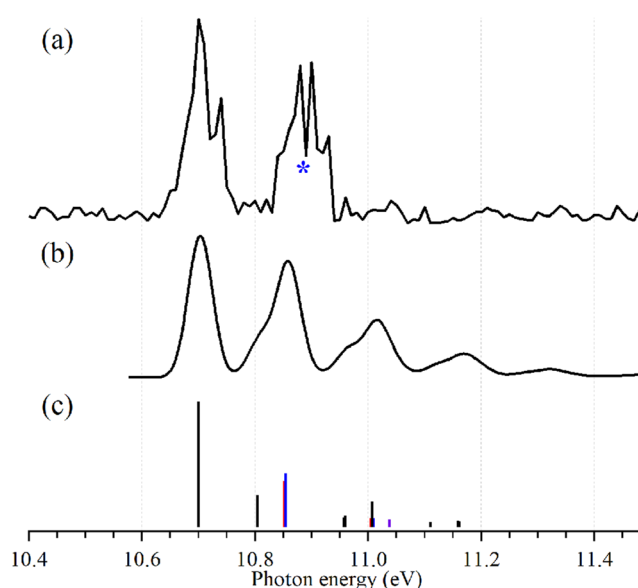


**FIG. 3.** (a) Experimental threshold photoelectron spectrum (TPES) of the  $\text{CH}_3\text{O}$  radical, (b) simulated PES, and (c) stick PES based upon calculated Franck–Condon factors.

intensities can be affected by the presence of autoionizations, the low signal-to-noise ratio in this region precludes further comment. The absolute photon energy of the TPES has been calibrated online with the AIEs of  $\text{H}_2\text{CO}$  ( $10.8887 \pm 0.0005$  eV) and the  $\text{CH}_3$  radical ( $9.838\,91 \pm 0.000\,19$  eV).<sup>33,34</sup> Therefore, the AIE of the  $\text{CH}_3\text{O}$  radical is determined from Fig. 3 at  $10.701 \pm 0.005$  eV, the error bar mainly including the uncertainty of the photon energy calibration and the influences of the scanning step size and the signal-to-noise ratio.<sup>35</sup> The AIE agrees reasonably well with the reported values of  $10.72 \pm 0.01$  eV<sup>6</sup> and  $10.78 \pm 0.02$  eV<sup>7</sup> for  $\text{CH}_3\text{O}$  with HeI PES. Furthermore, the M062X/aug-cc-pVTZ calculations in this work show that the difference in zero point energy (ZPE) in the neutral and cation between  $\text{CD}_3\text{O}$  and  $\text{CH}_3\text{O}$  places the AIE of the former 28 meV above that of the latter. This puts the present AIE( $\text{CH}_3\text{O}$ ) in good agreement with the ones obtained for the deuterated species (see Table I). Note that the present result reduces the uncertainty of the literature data by a factor of 2–4. Moreover, considering the Active Thermochemical Tables (ATcT) database recommended enthalpy of formation for the neutral  $\text{CH}_3\text{O}$  radical  $\Delta_f H_{0\text{K}}^0(\text{CH}_3\text{O}) = 28.85 \pm 0.29$  kJ mol<sup>−1</sup>,<sup>19</sup> the present AIE value leads to an enthalpy of formation for the  $\text{CH}_3\text{O}^+$  cation  $\Delta_f H_{0\text{K}}^0(\text{CH}_3\text{O}^+) = 1061.36 \pm 0.41$  kJ mol<sup>−1</sup>.

**TABLE II.** Calculated Franck–Condon (FC) factors of the  $X^2E \rightarrow X^3A_2$  ionizing transition of  $\text{CH}_3\text{O}$ .

$v^a$	0 <sup>0</sup>	6 <sup>1</sup>	3 <sup>1</sup>	2 <sup>1</sup>	6 <sup>1</sup> 3 <sup>1</sup>	6 <sup>1</sup> 2 <sup>1</sup>	3 <sup>2</sup>	3 <sup>1</sup> 2 <sup>1</sup>	2 <sup>2</sup>	1 <sup>1</sup>	6 <sup>1</sup> 3 <sup>1</sup> 2 <sup>1</sup>	3 <sup>2</sup> 2 <sup>1</sup>	3 <sup>1</sup> 2 <sup>2</sup>
Energy <sup>b</sup>	0	840.95	1229.2	1245.2	2070.1	2086.2	2458.3	2474.4	2490.4	2724.5	3315.3	3703.5	3719.6
FC	0.320	0.082	0.117	0.135	0.026	0.030	0.023	0.065	0.024	0.021	0.013	0.016	0.015

<sup>a</sup> $v^n$  corresponds to the  $X^2E(v=0) \rightarrow X^3A_2(v=n)$  ionizing transition.

<sup>b</sup>Calculated energies relative to the adiabatic ionization energy of  $\text{CH}_3\text{O}$ . Unit is cm<sup>−1</sup>.



The C–O stretching ( $\nu_3$ ) and to a lesser extent the C–H stretching ( $\nu_1$ ) modes of  $\text{CH}_3\text{O}^+$  are expected to be excited upon ionization.<sup>8,9</sup> The C–O stretching mode was observed in the HeI PES of Zhu *et al.*, and the vibrational frequency was reported at  $1950\text{ cm}^{-1}$ .<sup>7</sup> The C–H stretching frequency was reported at  $2469\text{ cm}^{-1}$  in the infrared photodissociation spectrum of the  $\text{CH}_3\text{O}^+-\text{Ar}$  complex.<sup>36</sup> As shown in Fig. 3, the  $\nu_3$  (C–O stretching, in red) and  $\nu_2$  (umbrella, in blue) vibrational modes of the  $\text{CH}_3\text{O}^+$  cation are calculated to be populated upon photoionization, together with the  $\nu_6$  ( $\text{H}_3\text{C}$ –O bending) and  $\nu_1$  (C–H stretching, in purple) vibrational excitations and their combinations. The experimental signal-to-noise ratio does not allow us to refine the calculated frequencies and Franck–Condon factors, but the overall good agreement validates the theoretical methodology.

In the TPES, extra peaks can be observed at  $h\nu = 10.740\text{ eV}$  and, to a lesser extent due to the lower signal,  $10.930\text{ eV}$ , as high energy shoulders of the two vibrational bands, almost with the same spacing ( $\sim 40\text{ meV}$ ) from the main peaks. Previous theoretical calculations predicted the Jahn–Teller splitting energy of the  $\text{X}^2\text{E}$  ground state of the  $\text{CH}_3\text{O}$  radical at  $\sim 270\text{ cm}^{-1}$  ( $33\text{ meV}$ ).<sup>10,11</sup> As the  $\text{H}_3\text{C}$ –O bending ( $\nu_6$ ) with the  $e$  vibrational mode is excited in the ionization process, the Jahn–Teller splitting might contribute somewhat to the two shoulder peaks, even if the limited S/N ratio precludes a detailed analysis.

#### IV. CONCLUSIONS

In conclusion, the VUV photoionization of the  $\text{CH}_3\text{O}$  radical has been investigated by using the state-of-the-art method of  $i^2\text{PEPICO}$  spectroscopy on the DESIRS beamline at SOLEIL. A fast flow tube combined with a microwave discharge generator was employed as a chemical reactor to initiate reactions and generate radicals. Almost all the reactants and products have been efficiently and sensitively probed in the photoionization mass spectrum to disentangle the embedded chemical reactions in the flow tube. The  $\text{CH}_3\text{O}$  radical is generated via the bimolecular reaction between  $\text{CH}_3$  and  $\text{CH}_3\text{O}_2$  and the self-reaction of  $\text{CH}_3\text{O}_2$ . Then, the  $\text{CH}_3\text{O}^+$  cation from direct ionization of the  $\text{CH}_3\text{O}$  radical is successfully detected close to its ionization threshold. The mass-selected TPES of the  $\text{CH}_3\text{O}$  radical within the energy range of  $9.7\text{ eV}$ – $11.5\text{ eV}$  is measured after removal of the  $^{13}\text{C}$ –isotopic formaldehyde  $\text{H}_2^{13}\text{CO}$  signal. With the aid of the calculated Franck–Condon factors, the vibrational excitations of the  $\text{CH}_3\text{O}^+$  cation have been assigned in the TPES and the AIE of the  $\text{CH}_3\text{O}$  radical is determined accurately at  $10.701 \pm 0.005\text{ eV}$ . The calculated ZPE difference in the neutral and cation between  $\text{CD}_3\text{O}$  and  $\text{CH}_3\text{O}$  leads to an AIE( $\text{CD}_3\text{O}$ ) of  $10.729\text{ eV}$ . More generally, as demonstrated in this manuscript, the present work provides a benchmark and strategy to get the spectral fingerprint for very dilute and elusive species in complex atmospheric and combustion reactions.

#### SUPPLEMENTARY MATERIAL

See the [supplementary material](#) for possible ongoing reactions in the flow tube (Table S1) and the optimized structure of  $\text{CH}_3\text{O}^+$  and its calculated vibrational frequencies (Fig. S1).

#### ACKNOWLEDGMENTS

This work was supported by the National Natural Science Foundation of China (Grant Nos. 21773249 and 91961123) and the International Partnership Program of the Chinese Academy of Sciences (Grant No. 116134KYSB20170048). C.F. is grateful to the CAS President's International Fellowship Initiative (Grant No. 2018VMA0055). The authors thank the SOLEIL staff for smoothly running the facility and providing beamtime under Proposal No. 20150802.

#### DATA AVAILABILITY

The data that support the findings of this study are available from the corresponding authors upon reasonable request.

#### REFERENCES

- 1 J. J. Orlando, G. S. Tyndall, and T. J. Wallington, "The atmospheric chemistry of alkoxy radicals," *Chem. Rev.* **103**, 4657 (2003).
- 2 R. J. Buszek, A. Sinha, and J. S. Francisco, "The isomerization of methoxy radical: Intramolecular hydrogen atom transfer mediated through acid catalysis," *J. Am. Chem. Soc.* **133**, 2013 (2011).
- 3 R. Atkinson, "Rate constants for the atmospheric reactions of alkoxy radicals: An updated estimation method," *Atmos. Environ.* **41**, 8468 (2007).
- 4 B. Long, J. L. Bao, and D. G. Truhlar, "Kinetics of the strongly correlated  $\text{CH}_3\text{O} + \text{O}_2$  reaction: The importance of quadruple excitations in atmospheric and combustion chemistry," *J. Am. Chem. Soc.* **141**, 611 (2019).
- 5 S.-C. Kuo, Z. Zhang, R. B. Klemm, J. F. Liebman, L. J. Stief, and F. L. Nesbitt, "Photoionization of hydroxymethyl ( $\text{CD}_2\text{OH}$  and  $\text{CD}_2\text{OD}$ ) and methoxy ( $\text{CD}_3\text{O}$ ) radicals: Photoion efficiency spectra, ionization energies, and thermochemistry," *J. Phys. Chem.* **98**, 4026 (1994).
- 6 J. Baker, J. M. Dyke, A. R. Ellis, and A. Morris, "Primary products of the reactions of fluorine atoms with  $\text{CH}_3\text{OH}$ ,  $\text{CH}_3\text{SH}$  and  $\text{CH}_3\text{OCH}_3$  studied with ultraviolet photoelectron spectroscopy," *J. Electron Spectrosc. Relat. Phenom.* **73**, 125 (1995).
- 7 X. J. Zhu, M. F. Ge, J. Wang, Z. Sun, and D. X. Wang, "First experimental observation on different ionic states of both methylthio ( $\text{CH}_3\text{S}$ ) and methoxy ( $\text{CH}_3\text{O}$ ) radicals," *Angew. Chem., Int. Ed.* **39**, 1940 (2000).
- 8 B. Ruscic and J. Berkowitz, "Photoionization mass spectrometric studies of the isomeric transient species  $\text{CD}_2\text{OH}$  and  $\text{CD}_3\text{O}$ ," *J. Chem. Phys.* **95**, 4033 (1991).
- 9 L. A. Curtiss, L. D. Kock, and J. A. Pople, "Energies of  $\text{CH}_2\text{OH}$ ,  $\text{CH}_3\text{O}$ , and related compounds," *J. Chem. Phys.* **95**, 4040 (1991).
- 10 A. V. Marenich and J. E. Boggs, "A model spin-vibronic Hamiltonian for twofold degenerate electron systems: A variational *ab initio* study of  $\text{X}^2\text{E CH}_3\text{O}$ ," *J. Chem. Phys.* **122**, 024308 (2005).
- 11 Z. Shao and Y. Mo, "Jahn–Teller effect in  $\text{CH}_2\text{DO/CHD}_2\text{O}(\text{X}^2\text{E})$ : Vibronic coupling of all vibrational modes," *J. Chem. Phys.* **138**, 244309 (2013).
- 12 N. D. K. Petraco, W. D. Allen, and H. F. Schaefer, "Fragmentation path for hydrogen atom dissociation from methoxy radical," *J. Chem. Phys.* **116**, 10229 (2002).
- 13 T. Baer and R. P. Tuckett, "Advances in threshold photoelectron spectroscopy (TPES) and threshold photoelectron photoion coincidence (TPEPICO)," *Phys. Chem. Chem. Phys.* **19**, 9698 (2017).
- 14 D. V. Chicharro, S. M. Poullain, L. Bañares, H. R. Hrodmarsson, G. A. García, and J.-C. Loison, "Threshold photoelectron spectrum of the  $\text{CH}_2\text{OO}$  Criegee intermediate," *Phys. Chem. Chem. Phys.* **21**, 12763 (2019).
- 15 G. A. García, B. K. Cunha de Miranda, M. Tia, S. Daly, and L. Nahon, "DELICIOUS III: A multipurpose double imaging particle coincidence spectrometer for gas phase vacuum ultraviolet photodynamics studies," *Rev. Sci. Instrum.* **84**, 053112 (2013).
- 16 X. Tang, G. A. García, and L. Nahon, "High resolution vibronic state-specific dissociation of  $\text{NO}_2^+$  in the  $10.0$ – $15.5\text{ eV}$  energy range by synchrotron double

imaging photoelectron photoion coincidence,” *Phys. Chem. Chem. Phys.* **22**, 1974 (2020).

<sup>17</sup>E. E. Ferguson, J. Roncin, and L. Bonazzola, “Heat of formation and bond energies of  $\text{H}_3\text{CO}^+$  and  $\text{H}_3\text{COOH}^+$  ions,” *Int. J. Mass Spectrom. Ion Processes* **79**, 215 (1987).

<sup>18</sup>J. M. Dyke, A. R. Ellis, N. Jonathan, N. Keddar, and A. Morris, “Observation of the  $\text{CH}_2\text{OH}$  radical in the gas phase by vacuum ultraviolet photoelectron spectroscopy,” *Chem. Phys. Lett.* **111**, 207 (1984).

<sup>19</sup>B. Ruscic and D. H. Bross, Active Thermochemical Tables (ATcT) values based on version 1.122g of the Thermochemical Network, 2019, available at <https://ATcT.anl.gov>; accessed 20 May 2020.

<sup>20</sup>L. Nahon, N. de Oliveira, G. A. Garcia, J.-F. Gil, B. Pilette, O. Marcouillé, B. Lagarde, and F. Polack, “DESIRS: A state-of-the-art VUV beamline featuring high resolution and variable polarization for spectroscopy and dichroism at SOLEIL,” *J. Synchrotron Radiat.* **19**, 508 (2012).

<sup>21</sup>G. A. Garcia, X. Tang, J.-F. Gil, L. Nahon, M. Ward, S. Batut, C. Fittschen, C. A. Taatjes, D. L. Osborn, and J.-C. Loison, “Synchrotron-based double imaging photoelectron/photoion coincidence spectroscopy of radicals produced in a flow tube: OH and OD,” *J. Chem. Phys.* **142**, 164201 (2015).

<sup>22</sup>X. Tang, G. A. Garcia, J.-F. Gil, and L. Nahon, “Vacuum upgrade and enhanced performances of the double imaging electron/ion coincidence end-station at the vacuum ultraviolet beamline DESIRS,” *Rev. Sci. Instrum.* **86**, 123108 (2015).

<sup>23</sup>X. Tang, X. Gu, X. Lin, W. Zhang, G. A. Garcia, C. Fittschen, J.-C. Loison, K. Voronova, B. Sztáray, and L. Nahon, “Vacuum ultraviolet photodynamics of the methyl peroxy radical studied by double imaging photoelectron photoion coincidences,” *J. Chem. Phys.* **152**, 104301 (2020).

<sup>24</sup>W. Tao, R. B. Klemm, F. L. Nesbitt, and L. J. Stief, “A discharge flow-photoionization mass spectrometric study of hydroxymethyl radicals ( $\text{H}_2\text{COH}$  and  $\text{H}_2\text{COD}$ ): Photoionization spectrum and ionization energy,” *J. Phys. Chem.* **96**, 104 (1992).

<sup>25</sup>NIST Chemistry WebBook, <http://webbook.nist.gov/chemistry/>; retrieved on May 21, 2020.

<sup>26</sup>E. Assaf, C. Schoemaeker, L. Vereecken, and C. Fittschen, “The reaction of fluorine atoms with methanol: Yield of  $\text{CH}_3\text{O}/\text{CH}_2\text{OH}$  and rate constant of the

reactions  $\text{CH}_3\text{O} + \text{CH}_3\text{O}$  and  $\text{CH}_3\text{O} + \text{HO}_2$ ,” *Phys. Chem. Chem. Phys.* **20**, 10660 (2018).

<sup>27</sup>G. A. Garcia, L. Nahon, and I. Powis, “Two-dimensional charged particle image inversion using a polar basis function expansion,” *Rev. Sci. Instrum.* **75**, 4989 (2004).

<sup>28</sup>Z. Wen, X. Tang, C. Wang, C. Fittschen, T. Wang, C. Zhang, J. Yang, Y. Pan, F. Liu, and W. Zhang, “A vacuum ultraviolet photoionization time-of-flight mass spectrometer with high sensitivity for study of gas-phase radical reaction in a flow tube,” *Int. J. Chem. Kinet.* **51**, 178 (2019).

<sup>29</sup>J. C. Pouilly, J. P. Schermann, N. Nieuwjaer, F. Lecomte, G. Grégoire, C. Desfrancis, G. A. Garcia, L. Nahon, D. Nandi, L. Poisson, and M. Hochlaf, “Photoionization of 2-pyridone and 2-hydroxypyridine,” *Phys. Chem. Chem. Phys.* **12**, 3566 (2010).

<sup>30</sup>M. Briant, L. Poisson, M. Hochlaf, P. de Pujo, M.-A. Gaveau, and B. Soep, “ $\text{Ar}_2$  photoelectron spectroscopy mediated by autoionizing states,” *Phys. Rev. Lett.* **109**, 193401 (2012).

<sup>31</sup>K. Voronova, K. M. Ervin, K. G. Torma, P. Hemberger, A. Bodi, T. Gerber, D. L. Osborn, and B. Sztáray, “Radical thermometers, thermochemistry, and photoelectron spectra: A PEPICO study of the methyl peroxy radical,” *J. Phys. Chem. Lett.* **9**, 534 (2018).

<sup>32</sup>M. J. Frisch, G. W. Trucks, H. B. Schlegel, G. E. Scuseria, M. A. Robb, J. R. Cheeseman, G. Scalmani, V. Barone, B. Mennucci, and G. A. Petersson, Gaussian 16, Revision B.01, Gaussian, Inc., Wallingford, CT, 2016.

<sup>33</sup>B. Niu, D. A. Shirley, and Y. Bai, “High resolution photoelectron spectroscopy and femtosecond intramolecular dynamics of  $\text{H}_2\text{CO}^+$  and  $\text{D}_2\text{CO}^+$ ,” *J. Chem. Phys.* **98**, 4377 (1993).

<sup>34</sup>A. M. Schulenburg, C. Alcaraz, G. Grassi, and F. Merkt, “Rovibrational photoionization dynamics of methyl and its isotopomers studied by high-resolution photoionization and photoelectron spectroscopy,” *J. Chem. Phys.* **125**, 104310 (2006).

<sup>35</sup>J. W. Brault, “High precision Fourier transform spectrometry: The critical role of phase corrections,” *Mikrochim. Acta* **3**, 215 (1987).

<sup>36</sup>J. D. Mosley, T. C. Cheng, A. B. McCoy, and M. A. Duncan, “Infrared spectroscopy of the mass 31 cation: Protonated formaldehyde vs methoxy,” *J. Phys. Chem. A* **116**, 9287 (2012).